

Fabriccio: Touchless Gestural Input on Interactive Fabrics

Te-Yen Wu¹, Shutong Qi^{1,2}, Junchi Chen^{1,3}, MuJie Shang^{1,4}

Jun Gong¹, Teddy Seyed⁵, Xing-Dong Yang¹

Dartmouth College¹, Beihang University², Shanghai Jiao Tong University³, WuHan University⁴,
Microsoft Research⁵

{te-yen.wu.gr; jun.gong.gr; xing-dong.yang}@dartmouth.edu, teddy@microsoft.com

ABSTRACT

We present Fabriccio, a touchless gesture sensing technique developed for interactive fabrics using Doppler motion sensing. Our prototype was developed using a pair of loop antennas (one for transmitting and the other for receiving), made of conductive thread that was sewn onto a fabric substrate. The antenna type, configuration, transmission lines, and operating frequency were carefully chosen to balance the complexity of the fabrication process and the sensitivity of our system for touchless hand gestures, performed at a 10 cm distance. Through a ten-participant study, we evaluated the performance of our proposed sensing technique across 11 touchless gestures as well as 1 touch gesture. The study result yielded a 92.8% cross-validation accuracy and 85.2% leave-one-session-out accuracy. We conclude by presenting several applications to demonstrate the unique interactions enabled by our technique on soft objects.

Author Keywords

Doppler Effect, Interactive Fabrics, Touchless Gesture.

CSS Concepts

• Human-centered computing ~ Interaction devices

INTRODUCTION

As computing becomes increasingly ubiquitous and blends into our everyday devices (e.g. thermostats or speakers), the need to bring interactivity to everyday objects, including those made of soft and lightweight fabrics (e.g., garments, toys, and furniture) has grown significantly. This need has led to advances in sensing techniques that enable input to be carried out on interactive fabrics, such as touching [38, 42, 47, 50] or deforming the fabric [39, 59].

However, a challenge with existing input modalities is that physical contact with fabric must occur during the interaction. Thus, opportunities are missed for users to utilize other methods, such as touchless (or mid-air) hand gestures, commonly seen on smartphones [23.], smart watches [19, 30, 61], car infotainment systems [10.], and smart IoT devices [24]. The touchless, mid-air gestures performed by a hand or fingers near a sensor, significantly extends the input

Permission to make digital or hard copies of all or part of this work for personal or classroom use is granted without fee provided that copies are not made or distributed for profit or commercial advantage and that copies bear this notice and the full citation on the first page. Copyrights for components of this work owned by others than ACM must be honored. Abstracting with credit is permitted. To copy otherwise, or republish, to post on servers or to redistribute to lists, requires prior specific permission and/or a fee. Request permissions from Permissions@acm.org.

CHI '20, April 25–30, 2020, Honolulu, HI, USA

© 2020 Association for Computing Machinery. ACM ISBN 978-1-4503-6708-0/20/04...\$15.00 <https://doi.org/10.1145/3313831.3376681>



Figure 1. Fabriccio enables touchless gesture sensing on interactive fabric. For example, by embedding Fabriccio into pants, a user can perform subtle arms-down gestures to interact with a phone.

vocabularies of interactive fabrics including those carrying special meaning that can't be replaced by touch (e.g., waving the hand for a greeting). Touchless gestures are also useful in common scenarios where physical contact with a fabric is undesirable by a user (e.g., the hands are unclean when eating or exercising).

In this paper, we bring near-field touchless gestural input to interactive fabric using doppler motion sensing. With our technique, soft objects augmented with a textile motion sensor can detect nearby finger gestures (e.g. in ~10 cm distance [19]) to trigger a desired application. This enables new types of interactions in a variety of contexts. For example, a plush dog toy can make a greeting sound to respond to a child's wave in front of it. When standing or walking, a user can perform micro finger gestures (e.g., sliding on the index finger using the thumb) with the hand hanging naturally alongside the body to discretely interact with a screen (Figure 1). This type of gesture is subtle, easy to perform, and can now be sensed through trousers, instead of needing heavy, leg mounted depth cameras which are used in current methods for such scenarios [31].

To demonstrate technical feasibility and application scenarios enabled by our technique, we developed a proof-of-concept prototype called Fabriccio (Figure 1). Our prototype was developed using a pair of loop antennas (one as a transmitter and the other as receiver) made of a conductive thread that was sewn onto a fabric substrate. The antenna type, configuration, and operating frequency were

carefully chosen to balance sensor sensitivity and the complexity and cost of the fabrication process, making it easy for the system to be adopted by other researchers and the maker community. Our prototype detects 10 touchless gestures, involving hand and finger motions in different scales. It can also detect the finger tapping the sensor. Results from an evaluation with 10 participants revealed 92.8% cross-validation accuracy and 85.2% leave-one-session-out accuracy.

Our contributions are: (1) a touchless gesture sensing technique for interactive fabrics that uses the Doppler effect; (2) a prototype demonstrating technical feasibility; (3) a study evaluating the accuracy our sensing technique; and (4) several applications to demonstrate the unique interactions enabled by our technique.

RELATED WORK

Our work intersects with previous research in three main areas: sensing technique for interactive fabrics, sensing techniques for touchless gestures, and textile antennas.

Sensing Input on Interactive Fabric

With current technologies, input techniques through interactive fabrics includes touch [38, 42, 47, 50], deformation [35, 39, 59], and object recognition [18, 43] using sensing techniques based on capacitance [21, 33, 39, 40, 41], resistance [37, 38, 43, 58, 66], and inductance [18].

Capacitive sensing is based on the effect of capacitive coupling and has been used in early explorations of sensing touch [24, 40, 41] and pressure [34] on smart fabrics. For example, the Musical Jacket [40] from MIT features a capacitive touch keypad made of stainless-steel yarns embroidered on denim for a user to provide touch input. This technique was later used in other research prototypes [21, 41] but has recently moved beyond research into commercial products. Project Jacquard [42] exemplifies a recent attempt to make the manufacturing process of capacitive sensing on fabrics scalable. With Project Jacquard, the electrodes of the sensor are created by weaving conductive yarn into a textile using a process compatible with the current industry standard.

Aside from capacitive sensing, techniques based on resistance are also common on smart fabrics. A textile resistive sensor has a three-layer structure involving a middle semi-conductive layer sandwiched between two conductor layers. eCushion [67] is an example of such an implementation. With resistive sensing, input is sensed based on the change detected in the resistance of the fabric when the fabric is compressed. A wide variety of applications have been developed using resistive sensing. For example, in Rofouei et al.'s work [44] the authors used a textile pressure sensor for object recognition based on the pressure footprint of different objects (e.g., weight and shape). eCushion [67] was developed for sensing the sitting posture of a user on a chair. GestureSleeve [50] allowed users to use touch gestures on the forearm to interact with a computing device. proCover

[27], an augmented prosthetic limb with pressure sensing capability uses a similar sensor. Recent advances in fabrication technique by Parzer et al. [38] allows the three-layer structure to be replaced by two thin threads.

Aside from resistance and capacitance, sensing techniques based on inductance have also been explored on fabrics. For example, Jun et al.'s work allows a metallic object to be recognized when an object is in contact with fabric [18]. The same technique can be used for sensing touch but the input resolution in a 2D space is limited due to the coarse arrangement of the sensor coils.

Our work differs from existing research in that it brings touchless gestural input, commonly found in games, TV, vehicles, mobile, and, wearable applications to interactive fabrics using Doppler motion sensing.

Sensing Touchless Gestural Input

Sensing techniques for touchless gestural input can be divided into those based on vision [52, 55, 60], radio frequency [30, 54, 57, 43, 49, 62, 69, 71, 73], pyroelectric infrared [19] and acoustics [20, 37, 64]. Cameras (both 2D and 3D) are also often used in a wide variety of applications. Examples include the work from Song et al. [56], which enables the sense of gestural input in a 3D space using a 2D camera, and the work from Wang et al. [60], which tracks 6DOF bimanual hand input using a depth camera. In addition to the vision-based approaches, techniques using radio frequency have also shown promise in sensing touchless hand (e.g. flicking, sliding, or hovering) [43, 54, 62] and finger gestures (e.g. pinching the thumb and index finger, pinching the thumb and pinky, sliding the thumb along the index finger, or rubbing the thumb and index finger) [19, 30, 49, 62]. Examples in this line of work include Mudra [70], which detects finger gestures using home Wi-Fi signals, and Soli [30, 62], which detects hand and finger gestures using 60 GHz radar signals. Our sensing technique is based on the Doppler effect, which has been shown effective in sensing hand motion as input for mobile devices [73]. Along with these methods, techniques based on pyroelectric infrared [19] and acoustics [20, 37, 64] are pushing the boundary of touchless gesture sensing. However, the challenge in adopting these methods on soft and thin fabrics is that existing methods are developed on traditional devices with a rigid body (e.g., the sensor is printed on a PCB) and thus do not immediately work on a fabric, and its subsequent integration limits the softness and breathability of the fabric.

Textile Antennas

Textile antennas made of conductive threads are an emerging technology in electrical engineering with applications primarily targeting wireless communication [6, 7, 9, 25, 36, 46, 65, 66], health monitoring [26, 46, 70], object identification [13, 51], and energy harvesting [17, 32]. For example, Roundjane et al.'s work [46] describes a spiral-shaped textile antenna stitched on a T-shirt for transmitting Bluetooth signals at a frequency of 2.4G Hz. Placed on the chest, a textile antenna can be used to sense the wearer's

breathing rates using Bluetooth and received signal strength indicator (RSSI). Shao et al. [51] proposed a textile RFID tag for object recognition. Loss et al. [32] developed a monopole antenna to harvest electromagnetic energy from the GSM and DCS signals in the environment.

Our work is novel in that we are the first to investigate how a textile antenna can be designed and developed for touchless gestural input. We identified the challenges unique to this problem and demonstrate a promising solution for a new set of smart fabric applications.

SENSING PRINCIPLE AND BACKGROUND

Doppler motion sensors are known for being cost-effective sensors for in-air gestures [16, 54, 69]. Its sensing principle is based on the Doppler effect, described as the shift in the frequency of a wave caused by the motion of an object (e.g., hand) in relation to the wave source. Most Doppler motion sensors have a transmitter and receiver, with each connecting to an antenna via transmission lines. The antennas are often placed next to each other at a certain distance. When operating, the transmitter supplies an electric current to the transmitting antenna, which radiates energy from the current as electromagnetic waves through the air. When there is a moving object near the sensor, the receiving antenna intercepts some of the power of the electromagnetic waves reflected by the object and produces an electric current to the receiver. The reflected signal is then mixed with the local signal of the baseband frequency, resulting in an intermediate frequency (IF) signal to allow the shift in the frequency of the reflected waves to be observed by an analog to digital converter (ADC) operates at low sampling rates.

The resolution of the frequency shift of the Doppler motion sensor is related to the operating frequency. The higher the operating frequency is, the more observable the shift in the reflected frequency will be. The sensitivity of the sensor is dependent on the signal-to-noise ratio (SNR), and often related to the strength of the received signal. In designing a textile Doppler motion sensor under a certain operating power, the antenna type, the distance between the antennas, and how the antennas are connected to the transmitter or receiver may significantly affect the sensitivity of the sensor. Our work strikes a balance between the sensitivity and fabrication cost and complexity.

SENSOR DESIGN

In this section, we present the design of our textile Doppler motion sensor based on four parameters: sensor operating frequency, antenna type, transmitting/receiving antenna configuration, and impedance matching.

Operating Frequency

For our implementation, we considered an operating frequency of 1 GHz and above for the sake of sensing resolution. In this range, three bandwidths are common in commercial Doppler sensors that comply with the FCC regulations [15]: X band (10.525 GHz), K band (24 G to 26 GHz), and V band (60 GHz to 67 GHz). The high frequency

antennas are in general good in resolution but extremely challenging to develop on fabric because of the level of precision needed in the fabrication process. For example, the diameter of a loop antenna running at 60 GHz must be made precisely at 1.59 mm (circumference of a loop antenna equals to wavelength). A small error of even +0.5 mm in diameter will shift the antenna’s operating frequency dramatically to 45.7 GHz [5]. To lower the fabrication complexity, we used the X band (10.525 GHz) in our exploration because the X band antennas are relatively larger in size and can be made in a level of precision that is achievable using a low-cost home embroidery sewing machine. We restricted our system to work at 3.3v, as we considered the capacity of the batteries in toys and wearable applications.

Antenna Design Options

For touchless gesture sensing, a desirable transmitting antenna design is one that can radiate a strong electromagnetic field above it. The challenge is that no existing knowledge provides an insight into the tradeoffs of the possible design options under our application requirements (e.g., X band, 3.3v, and near-field sensing). We thus conducted a simulation test, an approach commonly used in the design of textile antennas [29, 68].

We considered four common antenna types found in the literature [4, 25, 36, 45, 46], including dipole, loop, patch, and slot antenna. We created the candidate antennas in COMSOL [22] by following the size requirement for them to operate at 10.525 GHz (details later). Like prior work [48], we simulate the antenna using copper fabric (conductivity = 0.05 Ω /square). We are aware that the simulation may not replicate the antenna behavior on a real fabric, but the comparison using the estimation of the electric field served well for our decision making. Table 1 shows the electric field for each candidate in a 10 cm \times 10 cm space.

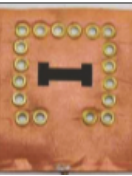
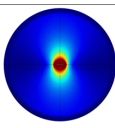
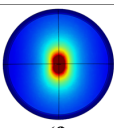
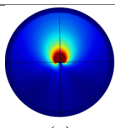
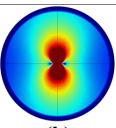
Antenna	Dipole	Loop	Patch	Slot
Type	Half-wave dipole	Large loop antenna	Patch antenna	Half-wave slot antenna
Photo				
	(a) [25]	(b) [46]	(c) [9]	(d) [36]
Electric Field				
	(e)	(f)	(g)	(h)

Table 1. The antennas and the electric field radiated by them in a 10 cm \times 10 cm space.

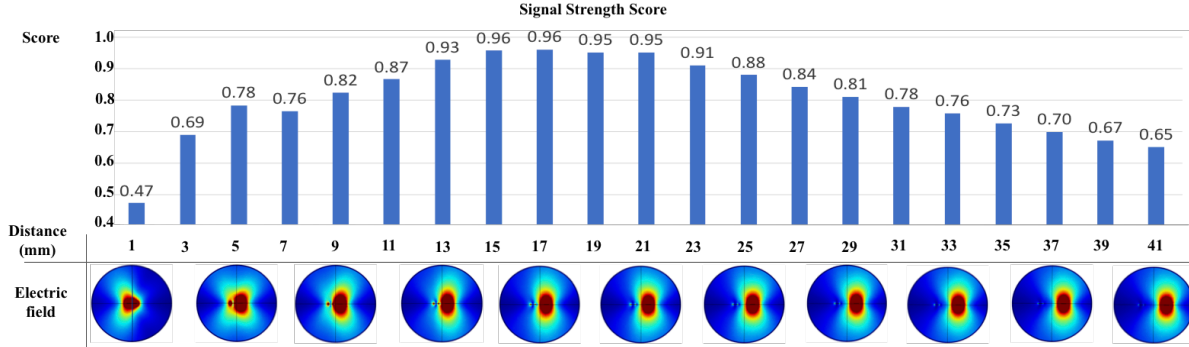


Figure 2. *Top*: the signal strength score of the reflected signal on the receiver. *Bottom*: the corresponding electric field at different antenna distances with a step size of 4 mm, indicating the interference from the receiving antenna.

Dipole antenna. The dipole antenna consists of two traces of equal length ($1/2$ wavelength), oriented end-to-end on a substrate. The structure of the dipole antenna is simple and can be made using conductive threads, embroidered onto a fabric [25] (Table 1a). However, the electric field of the dipole antenna appears to be the weakest amongst all four candidates.

Loop antenna. The loop antenna features a simple structure with a circular trace, where the circumference is equal to the wavelength of the operating frequency (28.5 mm in our case). Our simulation results suggest that the electric field of the loop antenna is stronger than dipole antenna. The loop antenna can also be fabricated using low-cost home embroidery sewing machine [46].

Patch antenna. The patch antenna consists of three layers, with the top and bottom layer made of a conductive plate, serving as the radiating and grounding plane respectively. The middle is an insulating dielectric layer. The size of the patch antenna at 10.525G Hz is $6.04 \text{ mm} \times 8.59 \text{ mm}$ [5]. The complexity of the three-layer structure, as well as the harsh material and thickness restriction for the insulation layer, makes it difficult to develop on fabric [46]. Table 1g shows that the strength of the electric field above the patch antenna is similar to that of the loop antenna.

Slot antenna. The slot antenna is made of a conductive surface with a slot cut out. The size of the slot antenna at 10.525G Hz is $14.25 \text{ mm} \times 1.34 \text{ mm}$ [5]. Table 1h suggests that the electric field radiated by the slot antenna is strongest of all the four candidates. The transmission lines of the slot antenna need to go through the center of the slot. Thus, an isolation layer needs to be placed between the transmission lines and the antenna.

Considering the balance between fabrication complexity and strength of the electric field, we chose the loop antenna in our implementation for both the transmitter and receiver. Note that the loop antenna is bidirectional, which means gestures can be sensed on both sides of the sensor, enabling new types of interactions. However, if only one direction is needed, an insulation layer can be used (more details later).

Transmitting and Receiving Antenna Configuration

The next step is to understand the impact of antenna configuration (or distance) on signal strength. If the antennas are placed too close to each other, the electric field of the transmitter may be interfered with the receiving antenna, thus weakening the signal. Moving the antennas away from each other can solve this problem but may also weaken the received signal. We thus conducted a second simulation test.

Simulation Setup

We studied 20 configurations with the antenna distance ranging from 1 mm to 41 mm, with a 2 mm step size. The distance was calculated using the closest points on the two loops. 1 mm was chosen as the closest distance because it is the closest that two threads can be stitched without touching each other using our embroidery machine. The other parameters, such as material type, remained the same as the first simulation study.

Since we were only interested in comparing the strength of the reflected signal, our simulation did not need a moving hand to create the reflection. Instead, we used a virtual circular copper plate above the antennas to create the reflection. We adjust the size of the plate to reflect the difference in the size of the hand and finger. Considering the average width of a hand [1] and finger [12], we used a plate of 10 cm and 1.8 cm wide for the hand and finger scenario respectively. Our data was collected with the copper plate placed at 5 cm or 10 cm above the sensor. The larger plate was positioned to cover both antennas, but the smaller plate was not big enough to cover both. Thus, we included three horizontal locations for the small plate, (1) the center of transmitting antenna, (2) the center of receiving antenna, and (3) the middle of the two antennas. In total, we sampled 20 distances \times 2 heights \times (1 location for the large plate + 3 locations for the smaller plate) = 160 data for test.

In COMSOL [22], the signal was represented using a complex number. Therefore, the strength of the reflected signal was calculated as the magnitude of the difference between the signal received with and without the copper plate. The collected data was then normalized across antenna distances and means (*signal strength score*) were calculated across the tested conditions for each antenna distance.

Results

We highlight the study results and the corresponding electrical field of the sensor with a step size of 4 mm in Figure 2. The peak of the signal occurred when the distance between the antennas was around 15 mm to 21 mm. The strength of the signal declines with the antenna distance exceeding 21 mm and beyond. On the other hand, the strength of the signal declines with a steeper slope before the peak, as the antenna distance is closer. This is due to the interference in the electric field from the receiving antenna. As shown in the bottom of Figure 2, the interference is clearly visible when the antenna distance is below 13 mm. To strike a balance between signal strength and sensor size, we chose 15 mm distance in our final design (Figure 3).

Impedance Matching and Transmission Line Routing

Energy loss may occur if there is a mismatch in the impedance of the antenna, its transmission line, and the transceiver [5]. Unfortunately, impedance match can hardly be guaranteed on a textile antenna and transmission lines [11]. We mitigated the issue by restricting the length of the transmission lines to a multiple of half of the wavelength of the operating frequency [5]. In our case, this method has an acceptable energy loss of around 11%, calculated using the formula of reflected power [3] with an antenna impedance of 100Ω [33], and source impedance of the transceiver of 50Ω (by most design). The challenge of this approach, however, is that sensor applications may require the antennas to be at any location on a substrate. When turns are made along the way toward the target location, the curve line is longer in the outer track of a turn than that in the inner track. As such, one transmission line will fail to satisfy the length requirement.

We solved this problem by including a semicircle and two quadrants in the track of the transmission line (Figure 3). The semicircle and quadrants should have the same radius, but their direction should be reversed to ensure that the total length of the inner and outer transmission lines is equal after turns occur. Assuming that in a coordinate system, where the origin is the terminal of the RF transceiver, given the location of the feed point (x, y) , the length of a transmission line connecting the origin and the feed point can be described as:

$$\frac{k \times \lambda}{2} = x + y + (\pi - 2)(2 \times r - g) + 2 \times l \quad (1)$$

where k is the factor, λ is the wavelength (28.5mm), r is the radius ($r < y$; 3 mm in our case), g is the distance between the two parallel transmission lines (1 mm), and l is the length of the line segment connecting the semicircle and a quadrant, which is the only unknown valuable in the equation. As l is the function of k , it can be calculated for any given k specified by a user using a variation of the Equation (1):

$$l = \frac{x+y+(\pi-2)(2 \times r-g)-\frac{k \times \lambda}{2}}{2} \quad (2)$$

The same approach can be used for two antennas. Figure 3 illustrates our implementation.

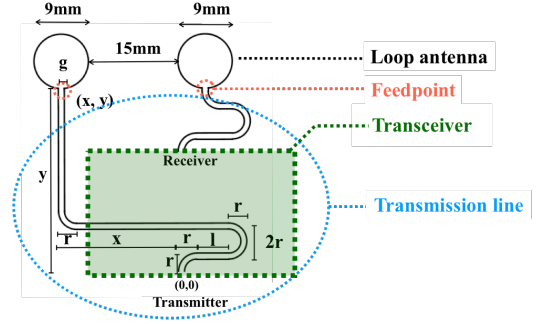


Figure 3. The final design for the antennas and transmission lines. The antenna design includes two loop antennas with a diameter of 9 mm and placed 15 mm away from each other. The design of transmission lines includes a semicircle, two quadrants, and several straight-line segments. A feed point distance of 1 mm was used for the parallel transmission lines.

IMPLEMENTATION

In this section, we discuss implementation details of the hardware and software.

Hardware

Conductive Thread Options

Another challenge of developing textile antennas is the choice of conductive threads. For example, the conductivity of the threads must be high, or energy loss may cause the reduction of the sensitivity. We found four conductive threads used in prior research [18] satisfy our needs (details in Table 2). Like in prior work [46], we estimate the performance of these threads using a simulation. We repeated our second test by simulating the antennas made by the candidate threads using the same thread conductivity. Our results showed no noticeable difference between the threads (Table 2). Considering that the higher conductivity the thread is, the less energy loss will occur in transmission, we used the LIBERATOR 40 in our implementation.

Name	Stainless thin thread	Smooth conductive thread	Conductive Thread Bobbin	LIBERATOR 40
Material	316L Stainless steel fiber	12UM Stainless steel fiber	316L Stainless steel fiber	Silver coated polymer
Thickness (mm)	0.20	0.12	0.35	0.18
Conductivity (Ω per m)	51.18	27.00	91.84	3.28
Signal Strength Score	0.96	0.99	0.91	1
Electric field				

Table 2. Different types of conductive yarns tested in our simulation with the corresponding electric field shown in a $10 \text{ cm} \times 10 \text{ cm}$ space.

Fabricating Textile Antennas

Once the antenna design and choice for the conductive thread is finalized, the textile antenna can be stitched using a standard home embroidery sewing machine (e.g. Brother SE600) on a fabric substrate (e.g. polyester in our case). We used stitching in our implementation as the antenna traces created using stitching can be mechanically stable and durable [18]. Note that the standard stitching process on an embroidery sewing machine pushes the conductive threads through the substrate, which may cause a short circuit if an insulation layer is used for unidirectional sensing. We adopted a method discussed in Dunneet. al.'s work [14] to overcome this challenge, where we carefully tuned the tension of the top thread (e.g. non-conductive thread) to ensure that the conductive thread only floats on the surface of the substrate without penetrating it (Figure 4).

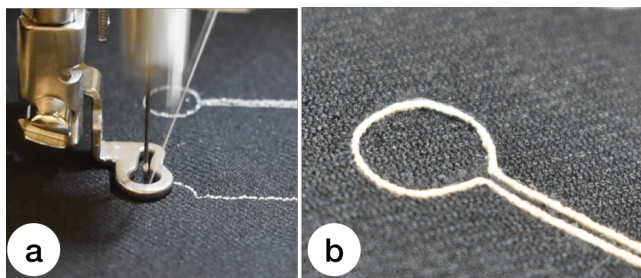


Figure 4. The fabrication of textile loop antennas. (a) Stitching textile antennas using a regular embroidery machine (b) The conductive thread floating on the surface of the substrate without penetrating it

Customized Sensing Board

Our customized sensing board is composed of a Doppler sensor board and a data collection board (Figure 5). The Doppler sensor board was modified from the HB100 Doppler Radar Motion Detector [55] by fully removing the patch antennas and the transmission line traces from the PCB, leaving only the RF transceiver component illustrated in Figure 5b. Ideally, the distance between the vias for the transmitter (or receiver) and ground should be the same as the antenna's feed-point distance (e.g., 1 mm), however this is not the case with our off-the-shelf device (e.g., 1.5 mm). This may affect sensitivity but can be fixed in the future with a fully customized board. The Doppler sensor board operates at a frequency of 10.525 GHz.

Our data collection board is a modification of an Adafruit Bluefruit LE Micro, which accommodates a differential amplifier circuit with a gain of 30 dB that amplifies the data received from the sensor board to the range of 0v to 3.3v, pin alignments for the sensor board, a micro-controller with a built-in 10bit ADC (TMEGA32U4), and a Bluetooth low energy module (nRF51822) for data transmission (Figure 5a). The data collection board was mounted on the sensor board with the entire system operating at 3.3v with a sampling rate of around 1000 Hz. All the sensor data was sent to a laptop for data processing. In total, the entire system consumes 158mW of power including those consumed by

the micro-controller and Bluetooth radio (45 mW). With a 400 mAh lithium-polymer battery, the system can work for approximately 2.5 hours. The cost of the sensing board is less than 30 dollars.

Wire Connection

Connecting the conductive threads to rigid electronics is an open problem in research that is yet to be solved [18, 38, 42]. Prior work has suggested methods, including soldering, using snap buttons, sewing, conductive epoxy, and crimping [8, 18, 38, 42]. Most of them except conductive epoxy, however, do not work in our case for varying reasons. For example, as suggested by [18], solder heat can make the connecting tip of a thread fragile, causing unstable connections between the transmission line and the vias. In our implementation, we used a low temperature solder paste [3]. We first push the tip of the thread into the via and then soldered it with the solder paste using a heat gun at a temperature of 140 °C. We also adhered the sensing board on the fabric to avoid parts moving at the connection points. Our initial test suggested that this type of connection was stable, and durable in our experiments.

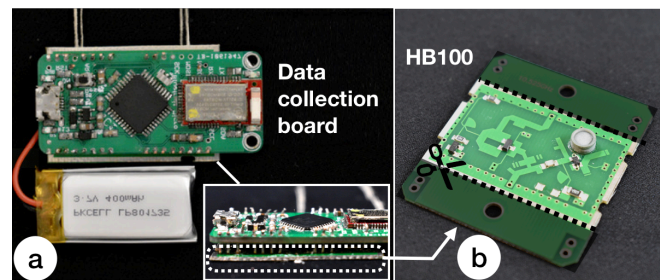


Figure 5. The customized sensing board, which consists of (a) a Doppler sensor board HB100 that is modified by removing antennas and transmission lines marked as dark areas and (b) a data collection board mounted on the modified HB100 sensor board with a 400 mAh battery.

Software

Signal Processing & Featurization

Sensor data was processed with a low-pass filter at 100Hz to remove the background noise. The features for machine learning were extracted in both frequency and time domains. For the features in the frequency domain, we first computed a frequency spectrum using a 90% overlapping, 240 window-sized FFT, which is then used to compute the max, mean, min, and standard deviation for each frequency band (20×4 values), resulting in 80 features for the classifier. In addition, we used a feature extraction toolbox (tsfresh [2]) to compute numbers of features in both frequency and time domain (e.g. continuous wavelet transform, the quantiles, binned entropy and etc.) In total, 480 features were fed into the machine learning model.

Machine Learning

To classify touchless gestures, we used the Random Forest from Scikit-learn with a forest size of 100 and the maximum depth of 30. We chose Random Forest because of its

accuracy in our initial tests rather than alternatives (e.g. SVM and Neural networks). The value of the parameters was chosen to balance the sensing accuracy and model complexity. We ran the classifier on a Microsoft Surface laptop. Table 3 shows the top-50 most effective and relevant features ranked by a Random Forest classifier using within-user model.

Time Domain (38)	Linear least-squares regression (13)
	Mean absolute change quantiles (8)
	Complexity-invariant distance (2)
	The unconditional maximum likelihood of an autoregressive process (2),
	Number of peaks (3)
	Binned entropy,
	Ratio beyond r sigma, energy ratio, maximum, minimum, autocorrelation, percentage of reoccurring datapoints, Friedrich coefficients, Kurtosis, absolute sum of changes.
Frequency Domain (12)	Fast Fourier Transform (11)
	FFT coefficient (1)

Table 3. Top-50 features ranked by Random Forest.

APPLICATIONS AND SCENARIOS

We created several demo applications to elucidate Fabriccio capabilities and highlight many of its usage scenarios in everyday furniture, clothing, and soft objects.

Interactive Furniture

The first application we implemented is an integrated media controller for a sofa, where a user controls the media playing on a TV, with gestures performed above an armrest. A swipe gesture can navigate the program, while a push gesture can pause or play media currently playing on the TV. In the scenarios where a user does not want to touch the sofa because their hands are unclean (e.g., when eating), the touchless hand gestures are useful additions to touch input on fabric (Figure 6).



Figure 6. Interactive furniture. A touchless remote control on the armrest of a sofa.

Interactive Clothing

Our second scenario involves turning everyday clothing into interactive wearables. For example, we augmented the logo of a sports shirt with Fabriccio to allow a user engaged in a

fitness activity to receive different types of audio information using gestures. For example, a user performing a check-mark gesture above a logo can be used for checking the percentage of their fitness goal, and similarly, a thumb circle gesture can be used for listening to their fitness schedule through the headphone, (Figure 7). In another example, we instrumented a pair of pants with Fabriccio on the side. This allows a user to perform subtle arms-down gestures alongside the body to interact with a smartphone (Figure 1).

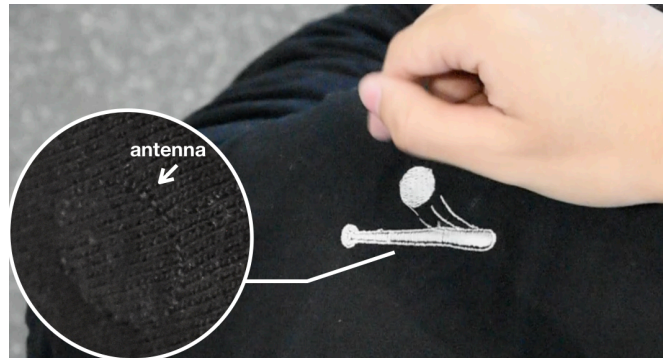


Figure 7 An interactive logo on a fitness shirt.

Interactive Soft Things

Finally, we demonstrate how Fabriccio can be useful in scenarios involving IoT-like devices by modifying everyday fabric-based objects. For some people, the backpack is a common part of life, and are used for carrying common objects, like smartphones. However, in some weather conditions (e.g. snow or rain) it is not ideal to take a smartphone out for simple tasks like answering a call or responding to notifications. We modified the two straps of a backpack by sewing and covering the sensors on each strap to allow for dual gesture input (Figure 8). For example, a circular gesture on the right strap allows the wearer to perform a circular gesture to listen their last text message when they are listening to music, while swiping near the left strap allows them to play and stop the music.



Figure 8. The straps of a backpack are modified by covering the sensors, which also allows for dual gestural input.

Interaction is also an important part of children's toys. We embedded Fabriccio into the head of a plush dog to enable simple interactive games for children. Waving the hand near the dog triggers a greeting sound. Touching its head plays a prompting sound (Figure 9).



Figure 9 Interactive plush toy for children. Waving the hand near the dog triggers a greeting sound. Touching its head plays a prompting sound.

EVALUATION

The goal of this study was to validate Fabriccio’s gesture recognition accuracy, as well as its robustness against individual variance and amongst different users.

Gesture Sets

To ensure that our exploration covered a wide variety of different type of touchless gestures, we surveyed existing work and chose 10 hand and finger motion gestures (Figure 10). Gestures selected varied in both motion trajectory and motion size, as many of the finger gestures, such as check mark and rectangle mark, are classified as micro gestures in the literature. We also included a touch gesture, which requires a user to tap the sensor.

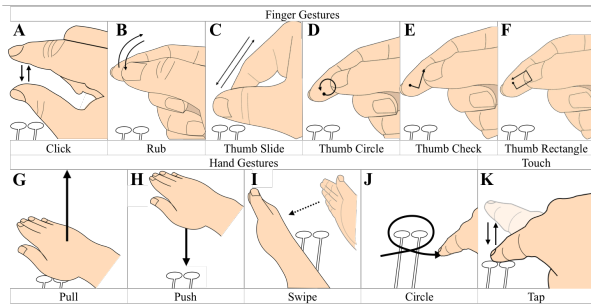


Figure 10. Our gesture set. Click, rub, thumb slide, swipe, pull, push, and circle were chosen from Soli [30, 62]; Thumb circle, check, and rectangle were chosen from Pyro [19].

Participants

Ten right-handed participants (average age: 21.6, 6 females) were recruited to participate in this study.

Data Collection

Each participant was instructed to sit in front of our textile sensor that was placed on a desk. Before a session started, participants were given several minutes to learn the 11 gestures. After a short training session, each participant performed a gesture toward the textile sensor, roughly in a distance between 5 to 10 cm using their right hand. The order of gestures was randomly assigned. The start and end of each gesture was indicated by clicking a computer mouse using their left hand. Each gesture was repeated 10 times in each session, which took about 30 minutes to complete. A 10-minute break was given between sessions, where participants

were asked to leave the desk and walk around the lab. Data collection finished after three sessions. In total, we collected 3300 samples ($10 \text{ participants} \times 11 \text{ gestures} \times 10 \text{ repetitions} \times 3 \text{ sessions}$) for analysis.

Results

To demonstrate the accuracy of our system, we present our result using within-user accuracy, cross-section accuracy and cross-user accuracy. Also, we computed the SNR for each gesture to demonstrate the sensitivity of our textile sensor.

Within-User Accuracy

Within-user accuracy is the measurement of the prediction accuracy where the training and testing data are from the same user. For each participant, we conducted a two-fold cross validation, where half of the data was used for training and the remaining data for testing. The overall within-user accuracy was calculated by averaging the results from all the participants. The result showed an accuracy of 92.8% (SD = 3.6%). Figure 11 left shows the confusion matrix. The major source of error was the confusion between the finger gestures with a similar motion. For example, *Click*, *Thumb slide* and *Thumb Check* accounted for the most misclassifications, as they all have two sharp turns in the motion trajectory.

Cross-Section Accuracy

Cross-section accuracy measured how stable the system was against the data collected from a different session. We calculated the leave-one-session-out accuracy for each participant by training the model using the data from the first two sessions and testing it using the last session. The overall across-section accuracy was the average of the accuracy from all participants. The results yielded an accuracy of 85.2% (SD = 10.4%). Figure 11 right shows the confusion matrix. Again, we found *Click* (82%), *Thumb slide* (76%) and *Thumb Check* (65.0%) contributed to the most errors. In addition, some finger gestures (e.g. *Thumb Rectangle*) began to cause confusions with others (e.g. *Rub* and *Thumb Check*). A potential reason is that the position and orientation in which the gestures were performed in relation to the sensor changed more significantly between sessions. We expect this issue can be mitigated with more training samples.

	A	B	C	D	E	F	G	H	I	J	K		A	B	C	D	E	F	G	H	I	J	K		
A	88.8	0.0	3.5	1.8	2.9	1.2	0.0	1.2	0.0	0.6	0.0		82.0	1.0	3.0	5.0	1.0	2.0	0.0	0.0	0.0	3.0	3.0	0.0	
B	0.0	95.9	0.0	0.0	0.0	0.0	0.0	0.0	0.7	3.4	0.0		0.0	91.0	1.0	0.0	4.0	0.0	2.0	0.0	0.0	1.0	1.0		
C	1.4	1.4	92.8	0.0	1.4	0.7	0.7	0.0	1.4	0.0	0.0		7.0	0.0	76.0	1.0	1.0	1.0	0.0	2.0	2.0	10.0	0.0	0.0	
D	0.6	0.0	2.5	88.8	1.2	5.6	0.0	0.0	0.0	1.2	0.0		5.0	0.0	4.0	84.0	4.0	3.0	0.0	0.0	0.0	0.0	0.0	0.0	
E	3.8	0.0	4.5	1.9	88.5	0.6	0.0	0.0	0.0	0.6	0.0		14.0	1.0	6.0	3.0	65.0	6.0	0.0	0.0	0.0	0.0	5.0	0.0	
F	2.2	0.7	0.0	0.7	1.5	94.2	0.0	0.7	0.0	0.0	0.0		2.0	2.0	0.0	7.0	10.0	0.0	0.0	2.0	0.0	0.0	0.0	0.0	
G	0.0	1.3	1.3	0.0	0.0	0.0	90.7	2.7	0.7	0.0	3.3		0.0	1.0	0.0	0.0	0.0	0.0	0.0	95.0	0.0	0.0	0.0	4.0	
H	0.0	0.0	0.7	0.0	0.0	0.0	2.1	95.2	0.0	1.4	0.7		0.0	1.0	1.0	0.0	0.0	0.0	3.0	92.0	0.0	1.0	2.0		
I	0.0	0.0	0.0	0.0	0.0	0.0	0.7	0.7	97.1	1.4	0.0		0.0	0.0	1.0	0.0	0.0	0.0	4.0	1.0	92.0	2.0	0.0		
J	0.0	3.8	1.3	1.3	0.0	0.0	0.0	0.0	0.0	93.6	0.0		0.0	3.0	0.0	1.0	0.0	5.0	0.0	0.0	2.0	89.0	0.0		
K	0.0	0.0	0.0	0.0	0.0	0.0	0.7	2.0	0.0	0.7	96.7		0.0	0.0	0.0	1.0	0.0	0.0	4.0	1.0	1.0	0.0	94.0		

Figure 11. Confusion matrix. Left: within-user accuracies. Right: leave-one-session-out accuracies

Cross-User Accuracy

Across-user accuracy measured whether an existing model works across different users. For the accuracy, we calculated

the leave-one-subject-out cross-validation accuracy by using the data from nine participants for training and the remaining one for testing. The overall accuracy is the average of the ten combinations of training and test data. The results yielded an accuracy of 65.5% (SD = 6.6%), indicating that the different users performed gestures differently. For example, some participants performed *Click* by moving both the thumb and index finger, while others only moved their index finger with the thumb staying in a relatively fixed position. Figure 12 shows the confusion matrix of all gestures. The most confusing gestures are *Click* (33.3%), *Thumb Check* (29.3%) and *Thumb Slide* (36.0%), followed by *Thumb Rectangle* (56.3%) and *Circle* (68.0%). We then removed them one by one and calculated the accuracies using the remaining data. The result yielded a higher accuracy of 75.3% (SD = 4.9%) without *Click* and *Thumb Rectangle*, and 87.6% (SD = 5.0%) without *Click*, *Thumb Check*, *Thumb Rectangle* and *circle*. This is encouraging, as the results showed that the differences in how the gestures (7 in our case) were performed across different people can be tolerated.

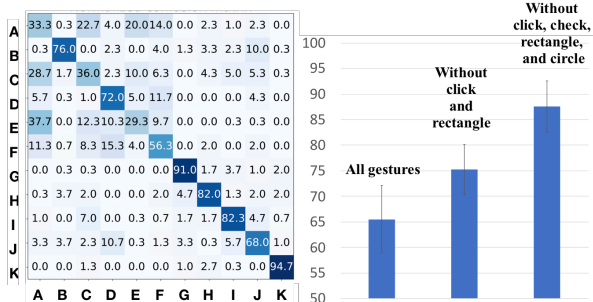


Figure 12. Left: confusion matrix of cross-user accuracies; Right: cross-user accuracy with different gesture sets.

Sensor Sensitivity

To validate the sensitivity of our textile sensor, we computed the SNR for the samples classified successfully in the within-user validation. As shown in Figure 13, the SNR for all the gestures were above 3dB, indicating that a minimum SNR of 3dB and above is needed for the sensor to reliably capture the gestures performed at a distance around 5cm to 10 cm.

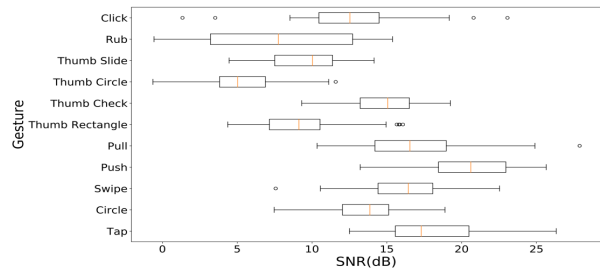


Figure 13. The box plot of the SNR for each gesture.

THE EFFECT OF COVERING FABRIC

In applications, where a fabric cover may be used on top of the sensor for design or aesthetic reasons, attenuation may occur due to occlusion and the sensor signal may become too weak to be used for reliable gesture recognition.

To explore this issue, we collected through-fabric sensor data using 17 fabrics made of acrylic, cotton, jute, linen, nylon, polyester, PVC leather, PU leather, faux fur, rayon, T-spun polyester, spun polyester, polypropylene, lyocell, olefin, modal rayon, and metallic yarns. We selected fabrics that are commonly found on garments, furniture, toys, and upholstery. We purposefully included those with varying thickness (0.17mm to 1.62mm) and materials (e.g. some have metallic threads). For each fabric, we measured the signal strength of our sensor in response to an object moving in a consistent pattern in front of it. We shielded the sensor on the back using a copper plate to avoid noise coming from the back. The consistency of the object movement across the tested fabrics is important to make an accurate comparison of the sensor signal. Our method for controlling the consistency was to use a motorized aluminum plate (20 cm × 20 cm) moving toward the sensor from a start position 6 cm away, stopping at 3 cm, and then moving back to the start position, achieved using an Ultimaker Original+ 3D printer. The tested fabric was placed on top of the sensor and tightened using a plastic frame.

Ten samples were collected for each fabric, with or without the presence of a covering fabric. A 1850 ms window, the movement time of the plate, was used for each sample to calculate the SNR. An average SNR was then calculated for each fabric per condition. The attenuation was calculated using the (logarithm) difference of the SNR with and without the fabric. It represents the ratio of the signal strength between two conditions. In total, we gathered 170 samples and we show the result in Figure 14.

The result showed that the fabrics woven with metallic thread caused a significant loss of signal (larger than 8db). As these fabrics could effectively block the signal of the sensor, we used them for shielding. Other types of fabric do not cause any significant attenuation of signal strength (within 2.17db). In reference to the results of our main evaluation, the attenuations of these fabrics are all lower than the variation of SNR for each gesture. It means that our model should be capable of handling such variation in the signal caused by the tested fabric. The effect of attenuation may slightly shorten the interaction range but may also not significantly drop the accuracy of our system either.

LIMITATIONS AND FUTURE WORK

In this section, we discuss the limitations of our work and propose potential directions for future research.

Effect of Body Motion. Sensor readings may be different if the antenna is in motion. For example, if a user is jogging, the training data acquired in a stationary condition may be insufficient for recognizing the same set of gestures because the relative motion between the hand and sensor has changed. This is not a problem unique to Fabriccio, as touch input on wearables has the same issue. Our next step is to investigate the effect of sensor motion caused by different user activities, identify the issues unique to touchless gesture sensing, and explore practical solutions.

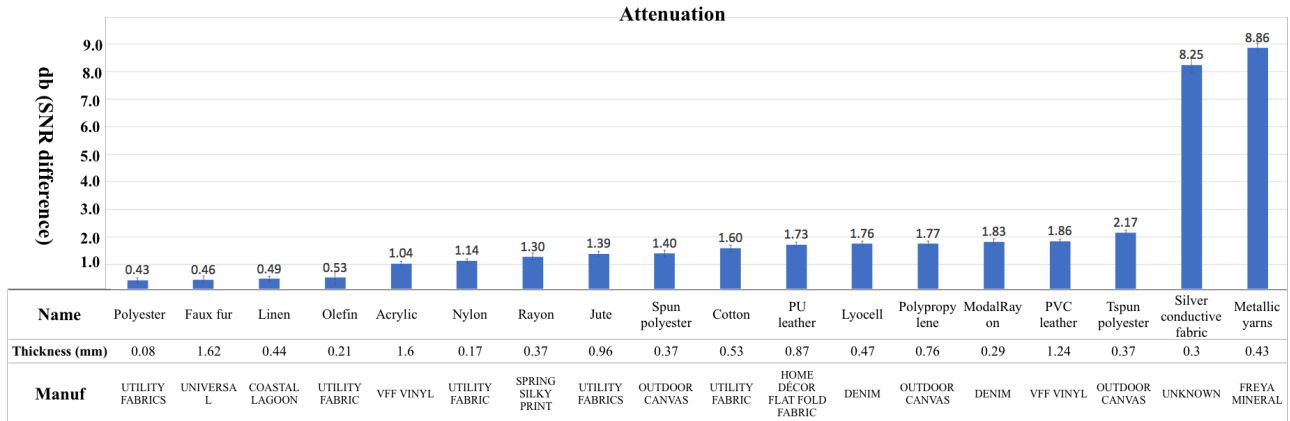


Figure 14. The attenuation effect of covering fabric.

Effect of Antenna Deformation. During our lab study and development of demo applications, we did not observe a noticeable impact on sensing performance when there was a small deformation in the antennas or transmission lines. However, we expect that antenna deformation, especially in large degrees, may eventually cause issues and affect the performance of the system on some of its applications. We plan to systematically investigate the change in the electric field and ultimately the recognition ability of the touchless gestures caused by antenna deformation. This will allow us to understand the challenges for the proposed sensing technique to be used in real-world scenarios and identify novel solutions to overcome the challenges.

Sensing Region and Range. Touchless gestures are required to be performed above the sensor. However, some applications may benefit from an extended ability for gesture sensing at any location on the fabric. The proposed sensor is not designed for this purpose. Our future work will continue in this direction. For example, we will develop an antenna array in a grid layout to enlarge the sensing region and even sense the coarse movement of the hand in a 2D space. Also, many challenges still exist, with one being the routing of the transmission lines and the interference of antennas.

Beyond Gesture Sensing. Radar technologies have found their way in many HCI applications, such as object recognition for tangible interactions [58] or activity sensing for context-aware applications [63]. Many of these technologies have great potential on daily objects covered or made of interactive fabrics. We will explore ways that can allow us to enable these novel interaction capabilities through ubiquitous textile antennas.

Energy Consumption. Our current implementation is powered using a battery. While sufficient for a research prototype in an early stage, it is expected that sensors of the future need to be self-sustainable. Textile antennas deliver this promise because they have been used for energy harvesting from radio waves in the environment (e.g., GSM) [17, 32]. It is thus possible to make our technique self-

powered for sensing or even data transformation [72]. We see it a fruitful direction for future research.

CONCLUSION

In this paper, we demonstrated the feasibility of recognizing touchless thumb-tip gestures on interactive fabrics using the Doppler effect. We developed a proof-of-concept prototype using a pair of antennas made of conductive thread sewn onto a fabric substrate. We carefully chose the antenna type, configuration, transmission lines, and operating frequency to balance the complexity of the fabrication process and the sensitivity of the system for touchless hand gestures. We demonstrate that our system can achieve a 92.8% cross-validation accuracy, and 85.2% cross-session accuracy in a user study with 10 participants and 11 touchless gestures as well as 1 touch gesture. For the subset of seven gestures, the cross-user accuracy can reach 87.6%. Our technique provides a useful addition to existing sensing techniques for user input on soft fabrics, primarily based on touch and deformation. This enables a new set of applications on everyday objects that are covered or made of interactive fabrics. We believe our technique may serve as important groundwork for integrating the gestural input into the soft objects in people's daily life.

REFERENCES

- [1] 2005. Glove Size. (2005). Retrieved August 14th from <https://www.davidmorgan.com/shop-content/glovesize/>.
- [2] 2017. tsfresh Toolkit. (2017). Retrieved August 14th from <https://tsfresh.readthedocs.io/en/latest/text/introduction.html>.
- [3] Amazon.com. No Clean Lead-Free Low Temperature Solder Paste 15 Grams. (9 November 2015). Retrieved August 14th from <https://www.amazon.com/Clean-Temperature-Solder-Paste-Grams/dp/B017RSGP18>
- [4] Dounia Baiya. 2014. On the Development of Conductive Textile Antennas.

- [5] Constantine A. Balanis. 2005. *Antenna Theory: Analysis and Design*. Wiley-Interscience, New York, NY, USA.
- [6] E. C. Bardera, M. Sánchez-Fernandez, L. A. Talegon and A. V. Delgado, "Feasibility of a wearable textile antenna hub based on massive MIMO systems," *2016 18th Mediterranean Electrotechnical Conference (MELECON)*, Lemesos, 2016, pp. 1-6. DOI: <http://dx.doi.org/10.1109/MELCON.2016.7495384>
- [7] Ashim Kumar Biswas and Ujjal Chakraborty. 2019. A compact wide band textile MIMO antenna with very low mutual coupling for wearable applications. *International Journal of RF and Microwave Computer-Aided Engineering* 29, 8, e21769. DOI: <http://dx.doi.org/10.1002/mmce.21769>
- [8] Leah Buechley and Michael Eisenberg. 2009. Fabric PCBs, electronic sequins, and socket buttons: techniques for e-textile craft. *Personal and Ubiquitous Computing* 13, 2, 133–150. DOI: <http://dx.doi.org/10.1007/s00779-007-0181-0>
- [9] Kuo-Sheng Chin, Chi-Sheng Wu, Chien-Lung Shen, and Kun-Chuan Tsai. 2018. Designs of Textile Antenna Arrays for Smart Clothing Applications. *Autex Research Journal* 18, 3, 295–307. DOI: <https://doi.org/10.1515/aut-2018-0002>
- [10] Continental Corporation. Gesture Recognition. Retrieved August 14th from <https://www.continental-automotive.com/en-gl/Passenger-Cars/Interior/Comfort-Security/Driver-Status/Gesture-Recognition>
- [11] D. Cottet, J. Grzyb, T. Kirstein, and G. Troster. 2003. Electrical characterization of textile transmission lines. *IEEE Transactions on Advanced Packaging* 26, 2 (May 2003), 182–190. DOI: <http://dx.doi.org/10.1109/TADVP.2003.817329>
- [12] Kiran Dandekar, Balasundar I. Raju, and Mandayam A. Srinivasan. 2003. 3-D Finite-Element Models of Human and Monkey Fingertips to Investigate the Mechanics of Tactile Sense. *Journal of Biomechanical Engineering* 125, 5 (10 2003), 682–691. DOI: <http://dx.doi.org/10.1115/1.1613673>
- [13] T. N. H. Doan, V. K. Nguyen, and N. C. Dao. 2016. A Textile Antenna for Wearable Applications Using RFID Technology. In *Proceedings of the 10th International Conference on Ubiquitous Information Management and Communication (IMCOM '16)*. ACM, New York, NY, USA, Article 73, 4 pages. DOI: <http://dx.doi.org/10.1145/2857546.2857621>
- [14] Lucy E. Dunne, Kaila Bibeau, Lucie Mulligan, Ashton Frith, and Cory Simon. 2012. Multi-layer e-Textile Circuits. In *Proceedings of the 2012 ACM Conference on Ubiquitous Computing (UbiComp '12)*. ACM, New York, NY, USA, 649–650. DOI: <http://dx.doi.org/10.1145/2370216.2370348>
- [15] FCC online table of frequency allocations. Retrieved August 14th from <https://transition.fcc.gov/oet/spectrum/table/fcctable.pdf>
- [16] T. Fan, C. Ma, Z. Gu, Q. Lv, J. Chen, D. Ye, J. Huangfu, Y. Sun, C. Li, and L. Ran. 2016. Wireless Hand Gesture Recognition Based on Continuous-Wave Doppler Radar Sensors. *IEEE Transactions on Microwave Theory and Techniques* 64, 11 (Nov 2016), 4012–4020. DOI: <http://dx.doi.org/10.1109/TMTT.2016.2610427>
- [17] A. Galoić, B. Ivšić, D. Bonefačić and J. Bartolić, "Wearable energy harvesting using wideband textile antennas," *2016 10th European Conference on Antennas and Propagation (EuCAP)*, Davos, 2016, pp. 1-5. DOI: <http://dx.doi.org/10.1109/EuCAP.2016.7481416>
- [18] Jun Gong, Yu Wu, Lei Yan, Teddy Seyed, and Xing-Dong Yang. 2019. Tessutivo: Contextual Interactions on Interactive Fabrics with Inductive Sensing. In *Proceedings of the 32st Annual ACM Symposium on User Interface Software and Technology (UIST '19)*. ACM, New York, NY, USA, 13. DOI: <http://dx.doi.org/10.1145/3332165.10.1145/3332165.3347897>
- [19] Jun Gong, Yang Zhang, Xia Zhou, and Xing-Dong Yang. 2017. Pyro: Thumb-Tip Gesture Recognition Using Pyroelectric Infrared Sensing. In *Proceedings of the 30th Annual ACM Symposium on User Interface Software and Technology (UIST '17)*. ACM, New York, NY, USA, 553–563. DOI: <http://dx.doi.org/10.1145/3126594.3126615>
- [20] Sidhant Gupta, Daniel Morris, Shwetak Patel, and Desney Tan. 2012. SoundWave: Using the Doppler Effect to Sense Gestures. In *Proceedings of the SIGCHI Conference on Human Factors in Computing Systems (CHI '12)*. ACM, New York, NY, USA, 1911–1914. DOI: <http://dx.doi.org/10.1145/2207676.2208331>
- [21] Paul Holleis, Albrecht Schmidt, Susanna Paasovaara, Arto Puikkonen, and Jonna Häkkinä. 2008. Evaluating Capacitive Touch Input on Clothes. In *Proceedings of the 10th International Conference on Human Computer Interaction with Mobile Devices and Services (MobileHCI '08)*. ACM, New York, NY, USA, 81–90. DOI: <http://dx.doi.org/10.1145/1409240.1409250>
- [22] COMSOL Inc. 2018. COMSOL Multiphysics Modeling Software. (3 October 2018). Retrieved August 14th from <https://www.comsol.com>

- [23] Google Inc. 2019. Pixel 4. (29 July 2019). Retrieved August 14th from <https://www.blog.google/products/pixel/new-features-pixel4/>.
- [24] Samsung Inc. Gesture Recognition. Retrieved August 14th from <https://www.samsung.com/in/support/tv-audio-video/what-is-gesture-control-in-samsung-f-series-smart-tv/>
- [25] T. Kaufmann, I. Fumeaux, and C. Fumeaux. 2013. Comparison of fabric and embroidered dipole antennas. In *2013 7th European Conference on Antennas and Propagation (EuCAP)*. 3252–3255.
- [26] A. Kiourti, C. W. L. Lee, J. Chae, and J. L. Volakis. 2016. A Wireless Fully Passive Neural Recording Device for Unobtrusive Neopotential Monitoring. *IEEE Transactions on Biomedical Engineering* 63, 1 (Jan 2016), 131–137. DOI: <http://dx.doi.org/10.1109/TBME.2015.2458583>
- [27] Joanne Leong, Patrick Parzer, Florian Perteneder, Teo Babic, Christian Rendl, Anita Vogl, Hubert Egger, Alex Olwal, and Michael Haller. 2016. proCover: Sensory Augmentation of Prosthetic Limbs Using Smart Textile Covers. In *Proceedings of the 29th Annual Symposium on User Interface Software and Technology (UIST '16)*. ACM, New York, NY, USA, 335–346. DOI: <http://dx.doi.org/10.1145/2984511.2984572>
- [28] Jacek Lesnikowski. 2011. Textile Transmission Lines in the Modern Textronic Clothes. *Fibres and Textiles in Eastern Europe* 89 (11 2011).
- [29] Yue Li, Zhijun Zhang, Zhenghe Feng, and Haider R. Khaleel. 2014. Fabrication and Measurement Techniques Of Wearable And Flexible Antennas.
- [30] Jaime Lien, Nicholas Gillian, M. Emre Karagozler, Patrick Amihood, Carsten Schwesig, Erik Olson, Hakim Raja, and Ivan Poupyrev. 2016. Soli: Ubiquitous Gesture Sensing with Millimeter Wave Radar. *ACM Trans. Graph.* 35, 4, Article 142 (July 2016), 19 pages. DOI: <http://dx.doi.org/10.1145/2897824.2925953>
- [31] Mingyu Liu, Mathieu Nancel, and Daniel Vogel. 2015. Gunslinger: Subtle Arms-down Mid-air Interaction. In *Proceedings of the 28th Annual ACM Symposium on User Interface Software & Technology (UIST '15)*. ACM, New York, NY, USA, 63–71. DOI: <http://dx.doi.org/10.1145/2807442.2807489>
- [32] Caroline Loss, Ricardo Gonçalves, Catarina Lopes, Pedro Pinho, and Rita Salvado. 2016. Smart Coat with a Fully-Embedded Textile Antenna for IoT Applications. *Sensors* 16, 6 (2016). DOI: <http://dx.doi.org/10.3390/s16060938>
- [33] Peter J. Massey, P. Fellows, Dariush Mirshekar-Syahkal, Arpan Pal, and Amit Mehta. 2016. *Loop Antennas*. Springer Singapore, Singapore, 723–786. DOI: http://dx.doi.org/10.1007/978-981-4560-44-3_26
- [34] J. Meyer, B. Arnrich, J. Schumm, and G. Troster. 2010. Design and Modeling of a Textile Pressure Sensor for Sitting Posture Classification. *IEEE Sensors Journal* 10, 8 (Aug 2010), 1391–1398. DOI: <http://dx.doi.org/10.1109/JSEN.2009.2037330>
- [35] Jussi Mikkonen and Riikka Townsend. 2019. Frequency-Based Design of Smart Textiles. In *Proceedings of the 2019 CHI Conference on Human Factors in Computing Systems (CHI '19)*. ACM, New York, NY, USA, Article 294, 12 pages. DOI: <http://dx.doi.org/10.1145/3290605.3300524>
- [36] Xing;Chen Maggie Yihong; Monne, Mahmuda Akter;Lan. 2018. Material Selection and Fabrication Processes for Flexible Conformal Antennas. *International Journal of Antennas and Propagation* 2018. DOI: <http://dx.doi.org/10.1155/2018/9815631>
- [37] Rajalakshmi Nandakumar, Vikram Iyer, Desney Tan, and Shyamnath Gollakota. 2016. FingerIO: Using Active Sonar for Fine-Grained Finger Tracking. In *Proceedings of the 2016 CHI Conference on Human Factors in Computing Systems (CHI '16)*. ACM, New York, NY, USA, 1515–1525. DOI: <http://dx.doi.org/10.1145/2858036.2858580>
- [38] Patrick Parzer, Florian Perteneder, Kathrin Probst, Christian Rendl, Joanne Leong, Sarah Schuetz, Anita Vogl, Reinhard Schwoedlauer, Martin Kaltenbrunner, Siegfried Bauer, and Michael Haller. 2018. RESi: A Highly Flexible, Pressure-Sensitive, Imperceptible Textile Interface Based on Resistive Yarns. In *Proceedings of the 31st Annual ACM Symposium on User Interface Software and Technology (UIST '18)*. ACM, New York, NY, USA, 745–756. DOI: <http://dx.doi.org/10.1145/3242587.3242664>
- [39] Patrick Parzer, Adwait Sharma, Anita Vogl, Jürgen Steimle, Alex Olwal, and Michael Haller. 2017. SmartSleeve: Real-time Sensing of Surface and Deformation Gestures on Flexible, Interactive Textiles, Using a Hybrid Gesture Detection Pipeline. In *Proceedings of the 30th Annual ACM Symposium on User Interface Software and Technology (UIST '17)*. ACM, New York, NY, USA, 565–577. DOI: <http://dx.doi.org/10.1145/3126594.3126652>
- [40] Alex P. Pentland. *Wearable Intelligence*. 90–95 pages.
- [41] E. R. Post, M. Orth, P. R. Russo, and N. Gershenfeld. 2000. E-broidery: Design and fabrication of textile-based computing. *IBM Systems Journal* 39, 3.4 (2000), 840–860. DOI: <http://dx.doi.org/10.1147/sj.393.0840>
- [42] Ivan Poupyrev, Nan-Wei Gong, Shiho Fukuhara, Mustafa Emre Karagozler, Carsten Schwesig, and Karen E. Robinson. 2016. Project Jacquard: Interactive Digital Textiles at Scale. In *Proceedings of the 2016 CHI Conference on Human Factors in Computing*

- Systems (CHI '16)*. ACM, New York, NY, USA, 4216–4227. DOI: <http://dx.doi.org/10.1145/2858036.2858176>
- [43] Qifan Pu, Sidhant Gupta, Shyamnath Gollakota, and Shwetak Patel. 2013. Whole-home Gesture Recognition Using Wireless Signals. In *Proceedings of the 19th Annual International Conference on Mobile Computing & Networking (MobiCom '13)*. ACM, New York, NY, USA, 27–38. DOI: <http://dx.doi.org/10.1145/2500423.2500436>
- [44] M. Rofouei, W. Xu, and M. Sarrafzadeh. 2010. Computing with uncertainty in a smart textile surface for object recognition. In *2010 IEEE Conference on Multisensor Fusion and Integration*. 174–179. DOI: <http://dx.doi.org/10.1109/MFI.2010.5604473>
- [45] Hendrik Rogier. 2015. *Textile antenna systems: Design, fabrication, and characterization*. 433–458. DOI: http://dx.doi.org/10.1007/978-981-4451-45-1_38
- [46] Mourad Roudjane, Mazen Khalil, Amine Miled, and Younés Messaddeq. 2018. New Generation Wearable Antenna Based on Multimaterial Fiber for Wireless Communication and Real-Time Breath Detection. *Photonics* 5, 4 (2018). DOI: <http://dx.doi.org/10.3390/photonics5040033>
- [47] Silvia Rus, Andreas Braun, and Arjan Kuijper. 2017. E-Textile Couch: Towards Smart Garments Integrated Furniture. In *Ambient Intelligence*. Springer International Publishing, Cham, 214–224. DOI: http://dx.doi.org/10.1007/978-3-319-56997-0_17
- [48] Rita Salvado, Caroline Loss, Ricardo Gonçalves, and Pedro Pinho. 2012. Textile Materials for the Design of Wearable Antennas: A Survey. *Sensors* 12, 11 (Nov 2012), 15841–15857. DOI: <http://dx.doi.org/10.3390/s121115841>
- [49] Y. Sang, L. Shi, and Y. Liu. 2018. Micro Hand Gesture Recognition System Using Ultrasonic Active Sensing. *IEEE Access* 6 (2018), 49339–49347. DOI: <http://dx.doi.org/10.1109/ACCESS.2018.2868268>
- [50] Stefan Schneegass and Alexandra Voit. 2016. GestureSleeve: Using Touch Sensitive Fabrics for Gestural Input on the Forearm for Controlling Smartwatches. In *Proceedings of the 2016 ACM International Symposium on Wearable Computers (ISWC '16)*. ACM, New York, NY, USA, 108–115. DOI: <http://dx.doi.org/10.1145/2971763.2971797>
- [51] S. Shao, A. Kiourti, R. J. Burkholder, and J. L. Volakis. 2015. Broadband Textile-Based Passive UHF RFID Tag Antenna for Elastic Material. *IEEE Antennas and Wireless Propagation Letters* 14 (2015), 1385–1388. DOI: <http://dx.doi.org/10.1109/LAWP.2015.2407879>
- [52] Toby Sharp, Cem Keskin, Duncan Robertson, Jonathan Taylor, Jamie Shotton, David Kim, Christoph Rhemann, Ido Leichter, Alon Vinnikov, Yichen Wei, Daniel Freedman, Pushmeet Kohli, Eyal Krupka, Andrew Fitzgibbon, and Shahram Izadi. 2015. Accurate, Robust, and Flexible Real-time Hand Tracking. In *Proceedings of the 33rd Annual ACM Conference on Human Factors in Computing Systems (CHI '15)*. ACM, New York, NY, USA, 3633–3642. DOI: <http://dx.doi.org/10.1145/2702123.2702179>
- [53] Kuldeep Kumar Singh. 2013. Review and Analysis of Microstrip Patch Array Antenna with different configurations.
- [54] S. Skaria, A. Al-Hourani, M. Lech, and R. J. Evans. 2019. Hand-Gesture Recognition Using Two-Antenna Doppler Radar With Deep Convolutional Neural Networks. *IEEE Sensors Journal* 19, 8 (April 2019), 3041–3048. DOI: <http://dx.doi.org/10.1109/JSEN.2019.2892073>
- [55] SMAKN. 2014. SMAKN HB100 Microwave Sensor Module 10.525GHz Doppler Radar Motion Detector. (7 May 2014). Retrieved August 14th from <https://www.amazon.com/SMAKN-Microwave-10-525GHz-Doppler-Detector/dp/B00FFW4AZ4>.
- [56] Jie Song, Gábor Sörös, Fabrizio Pece, Sean Ryan Fanello, Shahram Izadi, Cem Keskin, and Otmar Hilliges. 2014. In-air Gestures Around Unmodified Mobile Devices. In *Proceedings of the 27th Annual ACM Symposium on User Interface Software and Technology (UIST '14)*. ACM, New York, NY, USA, 319–329. DOI: <http://dx.doi.org/10.1145/2642918.2647373>
- [57] Li Sun, Souvik Sen, Dimitrios Koutsonikolas, and Kyu-Han Kim. 2015. WiDraw: Enabling Hands-free Drawing in the Air on Commodity WiFi Devices. In *Proceedings of the 21st Annual International Conference on Mobile Computing and Networking (MobiCom '15)*. ACM, New York, NY, USA, 77–89. DOI: <http://dx.doi.org/10.1145/2789168.2790129>
- [58] Klen Čopič Pucihar, Christian Sandor, Matjaž Kljun, Wolfgang Huerst, Alexander Plopski, Takafumi Taketomi, Hirokazu Kato, and Luis A. Leiva. 2019. The Missing Interface: Micro-Gestures on Augmented Objects. In *Extended Abstracts of the 2019 CHI Conference on Human Factors in Computing Systems (CHI EA '19)*. ACM, New York, NY, USA, Paper LBW0153, 6 pages. DOI: <https://doi.org/10.1145/3290607.3312986>
- [59] Anita Vogl, Patrick Parzer, Teo Babic, Joanne Leong, Alex Olwal, and Michael Haller. 2017. StretchEBand: Enabling Fabric-based Interactions Through Rapid Fabrication of Textile Stretch Sensors. In *Proceedings of the 2017 CHI Conference on Human Factors in Computing Systems (CHI '17)*. ACM, New York, NY,

- USA, 2617-2627. DOI:
<http://dx.doi.org/10.1145/3025453.3025938>
- [60] Robert Wang, Sylvain Paris, and Jovan Popovic'. 2011. 6D Hands: Markerless Hand-tracking for Computer Aided Design. In *Proceedings of the 24th Annual ACM Symposium on User Interface Software and Technology (UIST '11)*. ACM, New York, NY, USA, 549–558. DOI:
<http://dx.doi.org/10.1145/2047196.2047269>
- [61] Saiwen Wang, Jie Song, Jaime Lien, Ivan Poupyrev, and Otmar Hilliges. 2016a. Interacting with Soli: Exploring Fine-Grained Dynamic Gesture Recognition in the Radio-Frequency Spectrum. In *Proceedings of the 29th Annual Symposium on User Interface Software and Technology (UIST '16)*. ACM, New York, NY, USA, 851–860. DOI:
<http://dx.doi.org/10.1145/2984511.2984565>
- [62] Saiwen Wang, Jie Song, Jaime Lien, Ivan Poupyrev, and Otmar Hilliges. 2016b. Interacting with Soli: Exploring Fine-Grained Dynamic Gesture Recognition in the Radio-Frequency Spectrum. In *Proceedings of the 29th Annual Symposium on User Interface Software and Technology (UIST '16)*. ACM, New York, NY, USA, 851–860. DOI:
<http://dx.doi.org/10.1145/2984511.2984565>
- [63] Shuangquan Wang and Gang Zhou. 2015. A review on radio based activity recognition. *Digital Communications and Networks* 1, 1 (2015), 20 – 29. DOI: <https://doi.org/10.1016/j.dcan.2015.02.006>
- [64] Wei Wang, Alex X. Liu, and Ke Sun. 2016. Device-free Gesture Tracking Using Acoustic Signals. In *Proceedings of the 22Nd Annual International Conference on Mobile Computing and Networking (MobiCom '16)*. ACM, New York, NY, USA, 82–94. DOI: <http://dx.doi.org/10.1145/2973750.2973764>
- [65] Z. Wang, L. Z. Lee and J. L. Volakis, "A 10:1 bandwidth textile-based conformal spiral antenna with integrated planar balun," *2013 IEEE Antennas and Propagation Society International Symposium (APSURSI)*, Orlando, FL, 2013, pp. 220-221. DOI: <http://dx.doi.org/10.1109/APS.2013.6710771>
- [66] Z. Wang, L. Zhang, Y. Bayram, and J. L. Volakis. 2012. Embroidered Conductive Fibers on Polymer Composite for Conformal Antennas. *IEEE Transactions on Antennas and Propagation* 60, 9 (Sep. 2012), 4141–4147. DOI:
<http://dx.doi.org/10.1109/TAP.2012.2207055>
- [67] W. Xu, M. Huang, N. Amini, L. He, and M. Sarrafzadeh. 2013. eCushion: A Textile Pressure Sensor Array Design and Calibration for Sitting Posture Analysis. *IEEE Sensors Journal* 13, 10 (Oct 2013), 3926–3934. DOI:
<http://dx.doi.org/10.1109/JSEN.2013.2259589>
- [68] N. S. M. Yaziz and M. K. A. Rahim. 2015. Wideband textile antenna for wearable application. In *2015 IEEE International RF and Microwave Conference (RFM)*. 132–135. DOI:
<http://dx.doi.org/10.1109/RFM.2015.7587729>
- [69] Jiajun Zhang, Jinkun Tao, Jiangtao Huangfu, and Zhiguo Shi. 2017. Doppler-Radar Based Hand Gesture Recognition System Using Convolutional Neural Networks. *CoRR* abs/1711.02254 (2017).
<http://arxiv.org/abs/1711.02254>
- [70] L. Zhang, Z. Wang, and J. L. Volakis. 2012. Textile Antennas and Sensors for Body-Worn Applications. *IEEE Antennas and Wireless Propagation Letters* 11 (2012), 1690–1693. DOI:
<http://dx.doi.org/10.1109/LAWP.2013.2239956>
- [71] Ouyang Zhang and Kannan Srinivasan. 2016. Mudra: User-friendly Fine-grained Gesture Recognition Using WiFi Signals. In *Proceedings of the 12th International Conference on Emerging Networking EXperiments and Technologies (CoNEXT '16)*. ACM, New York, NY, USA, 83–96. DOI:
<http://dx.doi.org/10.1145/2999572.2999582>
- [72] Yang Zhang, Yasha Iravantchi1, Haojian Jin1, Swarun Swarun, and Chris Harrison1. 2019. Sozu: Self-Powered Radio Tags for Building-Scale Activity Sensing. In *Proceedings of the 32st Annual ACM Symposium on User Interface Software and Technology (UIST '19)*. ACM, New York, NY, USA, 13. DOI: <https://doi.org/10.1145/3332165.3347952>
- [73] Chen Zhao, Ke-Yu Chen, Md Tanvir Islam Aumi, Shwetak Patel, and Matthew S. Reynolds. 2014. SideSwipe: Detecting In-air Gestures Around Mobile Devices Using Actual GSM Signal. In *Proceedings of the 27th Annual ACM Symposium on User Interface Software and Technology (UIST '14)*. ACM, New York, NY, USA, 527–534. DOI:
<http://dx.doi.org/10.1145/2642918.2647380>